Observation of magnetic reconnection around a 3D null point

P. Romano[1], S.L. Guglielmino[2], M. Falco[1], M. Murabito[3].

[1] INAF - Osservatorio Astrofisico di Catania
[2] Università di Catania
[3] INAF - Osservatorio Astronomico di Roma

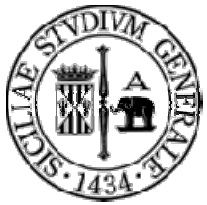

The location, the shape, and the motion of the flare ribbons provide useful information to understand the connectivity of the magnetic systems involved by the flare.

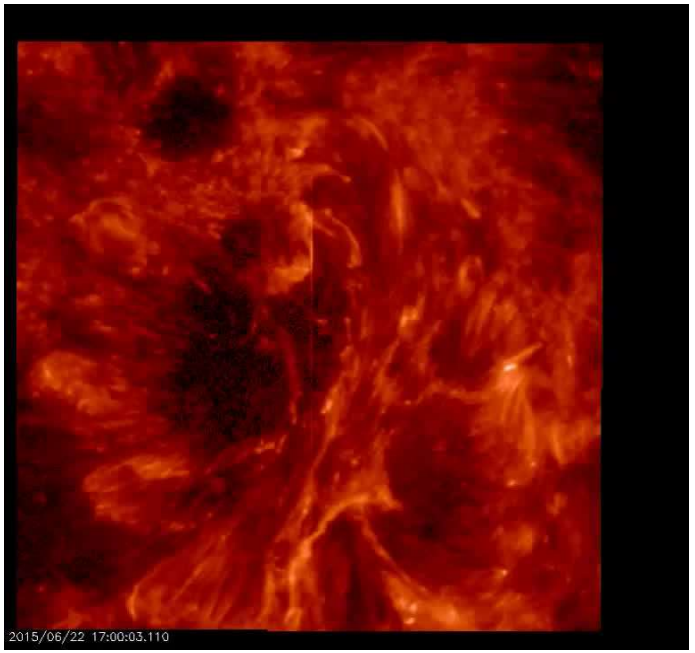

Sometimes the ribbons show a peculiar shape, which suggests some idea of the overlying topology of the magnetic field and an indication of the main reconnection site.

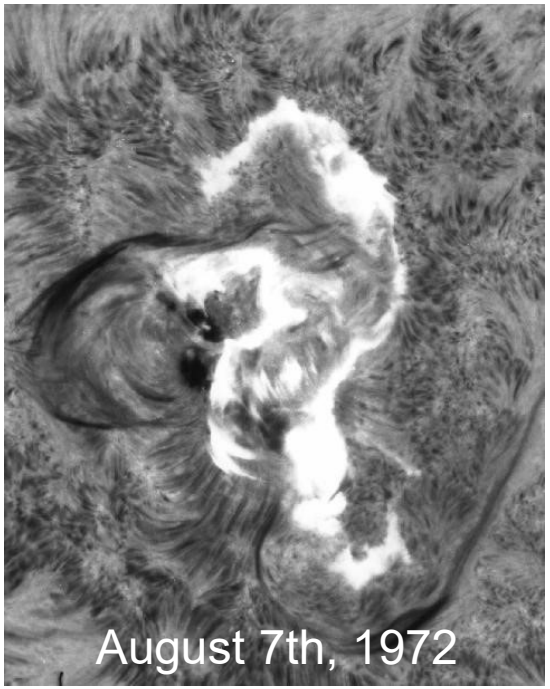

Circular ribbons

It is not easy to observe this kind of ribbon, probably due to the asymmetry of the real configuration and to the privileged direction of particle acceleration.

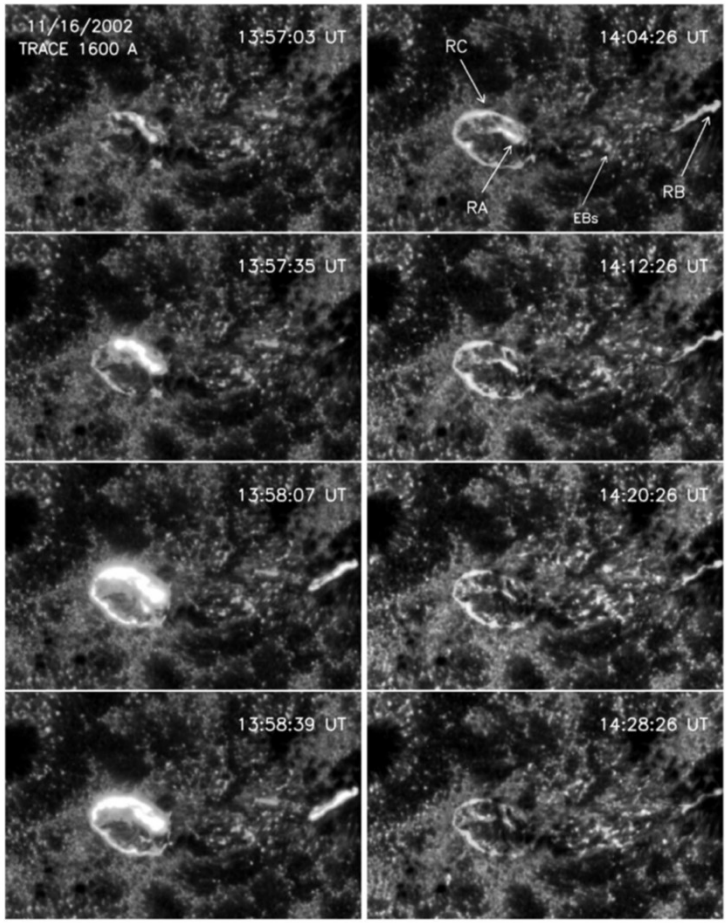

Masson et al. (2009)

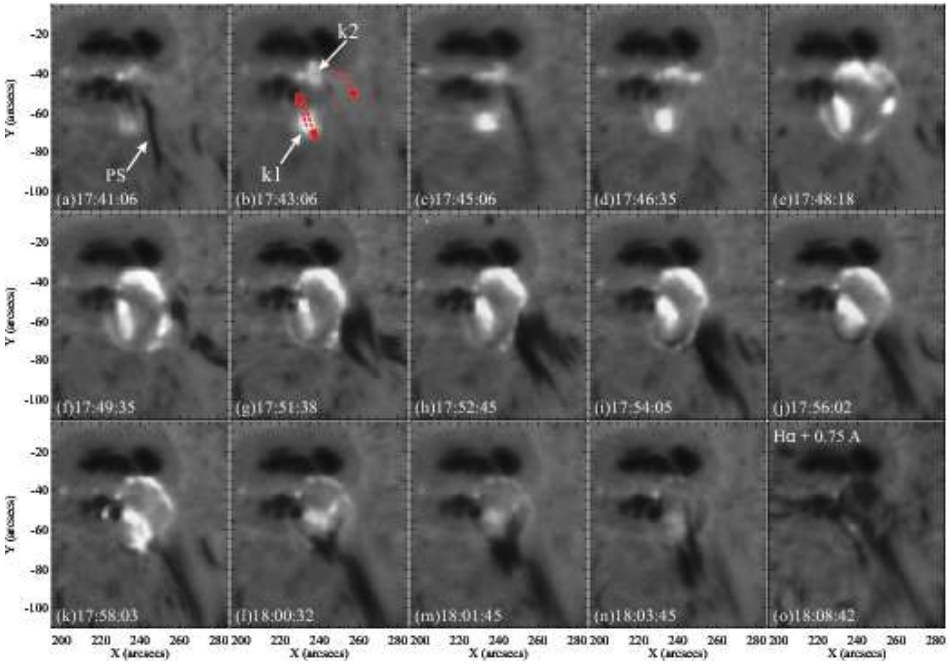

Wang & Liu (2012) observed a central parasitic magnetic field encompassed by the opposite polarity, forming a circular polarity inversion line traced by filament material.

3-D null points

Circular ribbons are often interpreted as the evidence of the presence in corona of a three-dimensional (3-D) null point.

The presence of a 3-D null point determines the formation of a surface, called fan, which divides the volume into two regions having a distinct connectivity.

The null point also originates two singular field lines, called the inner and outer spine, each of them belonging to one connectivity domain.

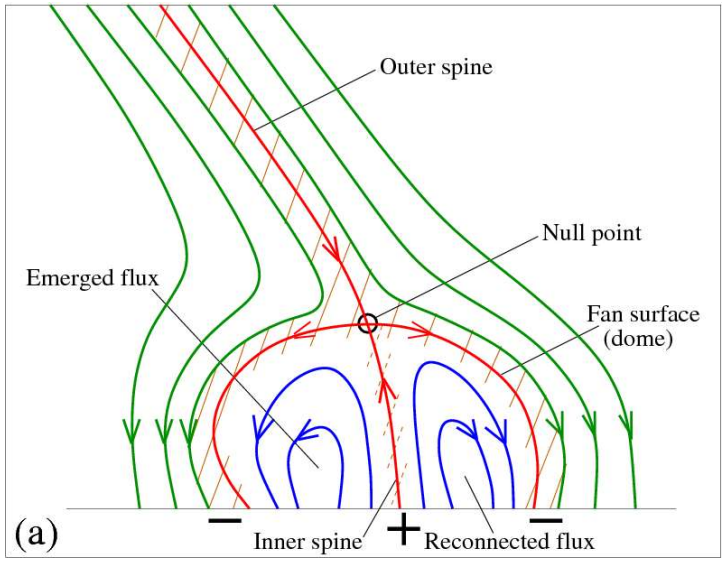

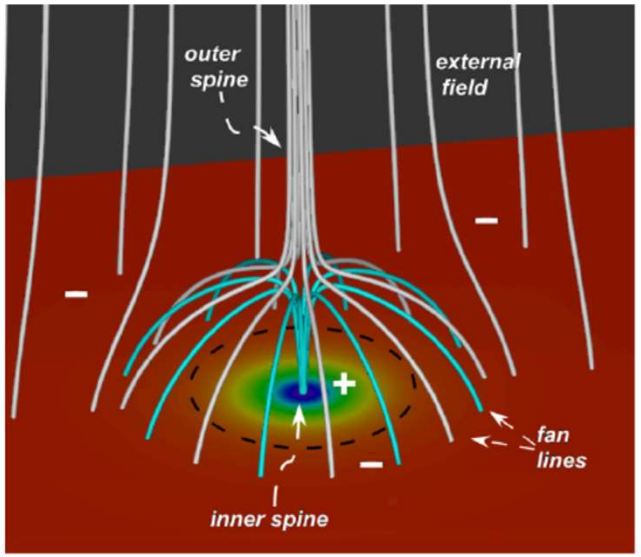

These separatrix field lines define preferential sites for the formation of current sheets and thus for magnetic reconnection: *spine reconnection* and *fan reconnection* (Priest & Titov, 1996).

Pontin et al. (2013), simulating the effect of a spine-fan magnetic reconnection process at a coronal null point by means of analytical and computational models, observed that the flipping of magnetic field lines in a manner similar to that observed in quasi-separatrix layers or the slip-running reconnection may occur in such a magnetic configuration.

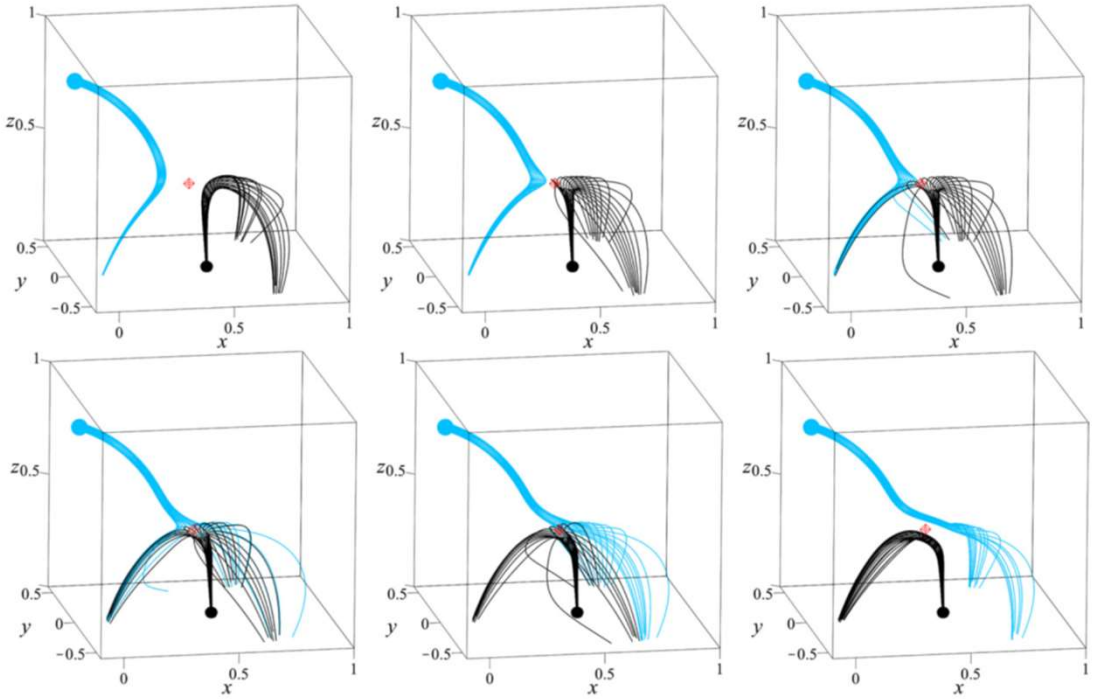

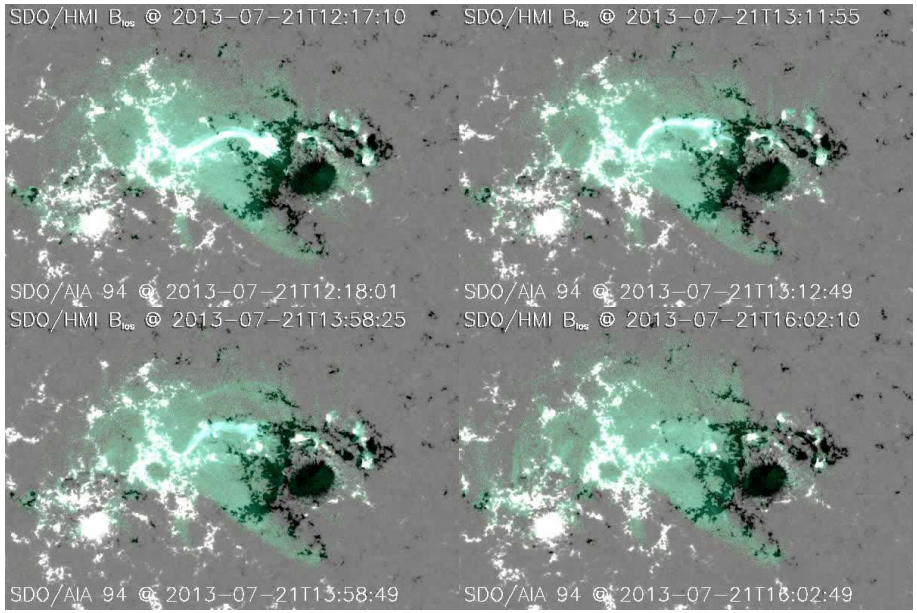

The slipping/slip-running reconnection in a fan-spine magnetic topology also seems to be associated with the occurrence of homologous jets, as observed by Wang & Liu (2012) and by Cheung et al. (2015), and the multiple-ribbon formation (e.g., Guglielmino et al. 2016).

Two length scales characterize the system: the width (N) of the jet source region and the footpoint separation (L) of the coronal loop that envelops the jet source.

Wyper & DeVore (2016) found that both the conditions for initiation and the subsequent dynamics of jets are highly sensitive to the ratio L/N.

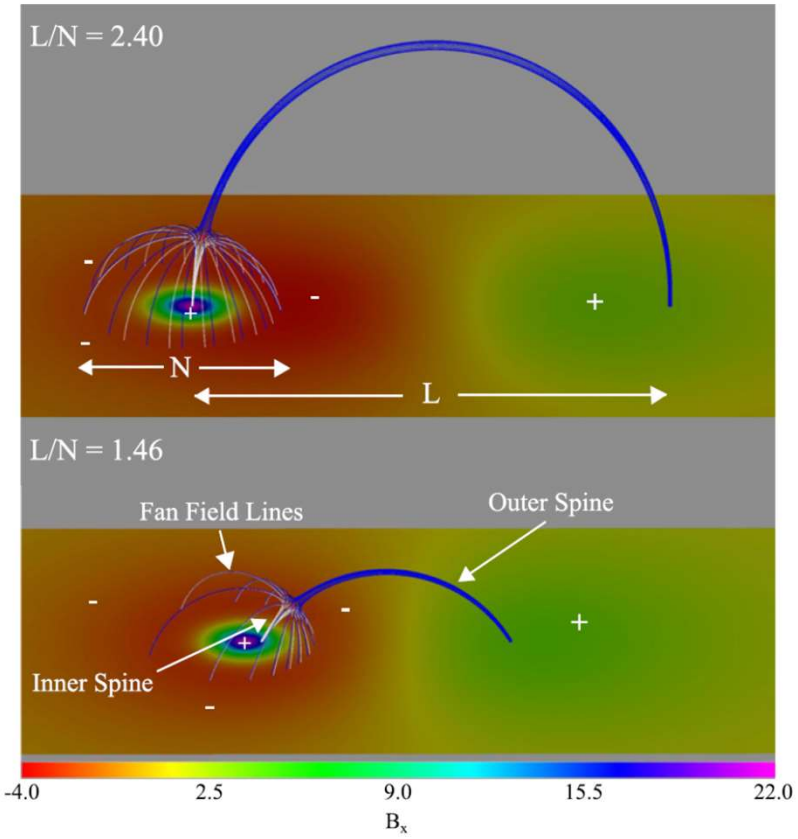

The longest-lasting and most energetic jets occur along long coronal loops with large L/N ratios, while smaller L/N ratios produce shorter-duration, less energetic jets

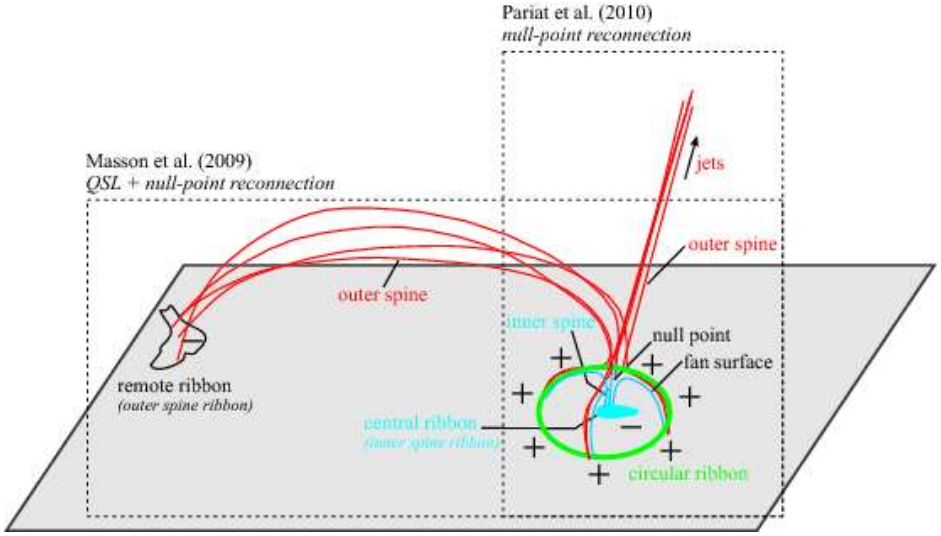

By flipping the outer spine field lines to open outward, one could arrive at an axisymmetrical null-point and fan-spine topology, which Pariat et al. (2009) used to model solar polar jets.

In the model of Pariat et al. (2009), the imposed twisting motion within the fan circle at the photospheric boundary builds up magnetic stress, until an ideal instability sets in to cause interchange reconnection at the null, driving massive, high-speed jets.

The numerical investigation was then extended in Pariat et al. (2010) by tilting the outer spine to break the axisymmetry and applying a constant stress to both closed- and open-connectivity domains.

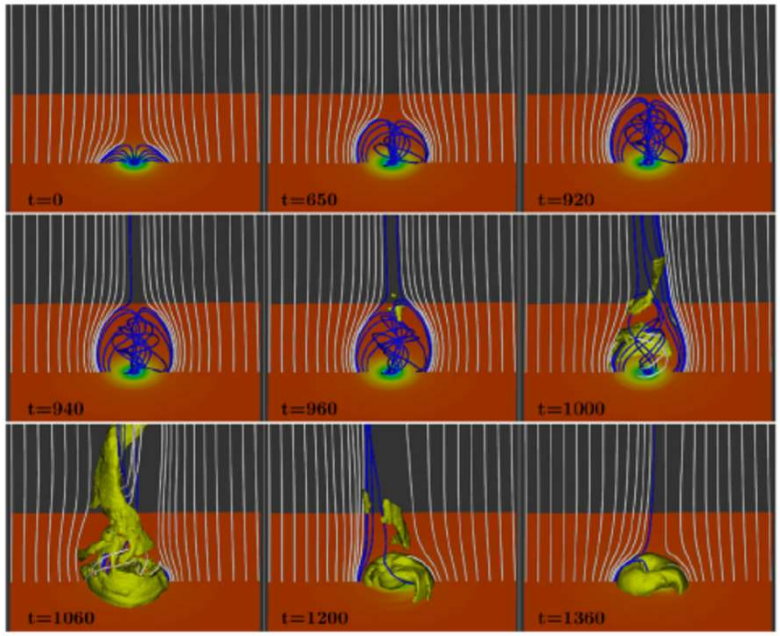

Under these prescribed perturbations, it was then shown that 3D null-point topology can naturally produce successive, homologous jets.

Our dataset

IBIS

Ca II 854.2 nm (25 spectral points)
Hα 656.28 nm (17 spectral points)
Fe I 617.3 nm (24 spectral points – 4 Stokes parameters)
Fe I 630.25 nm (30 spectral points – 4 Stokes parameters)

FOV: 500 x 1000 pixels
Pixel scale: 0.095”
Time spent for each scan: 67 s

Simultaneous broadband (633.32 ± 5 nm) counterpart imaging the same FOV with the same exposure time.

ROSA

393.3 nm (Ca II K), 417.0 nm (continuum), 486.1 nm (Hβ) and Gband.

FOV: 512 x 512 pixels
Spatial resolution: ~ 0.15”
Time cadence: 0.25 s

A small B GOES class flare occurred on May 20, 2015, in AR NOAA 12351

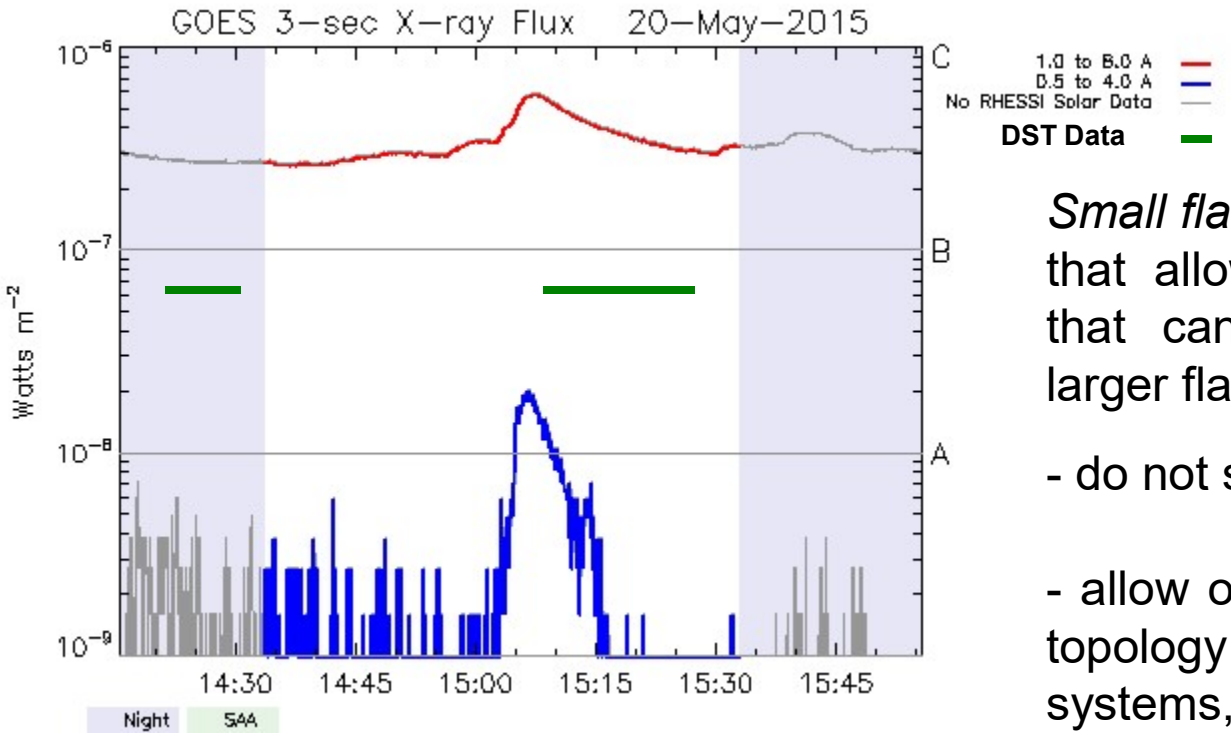

Small flares have some advantages that allow studying some aspects that cannot be investigated with larger flares:

- do not saturate the digital images

- allow one to observe in detail the topology of the involved magnetic systems, such as the flare loop configuration or the ribbon shape.

- have the advantage that they could be observed entirely within the FOV of high-resolution instruments.

The AR was located at about N22 E42

We observed at DST (IBIS-ROSA):

10 scans from 14:21 UT to 14:31 UT (before the flare onset)

20 scans from 15:09 UT to 15:30 UT (main phase)

AR NOAA 12351 observed by SDO

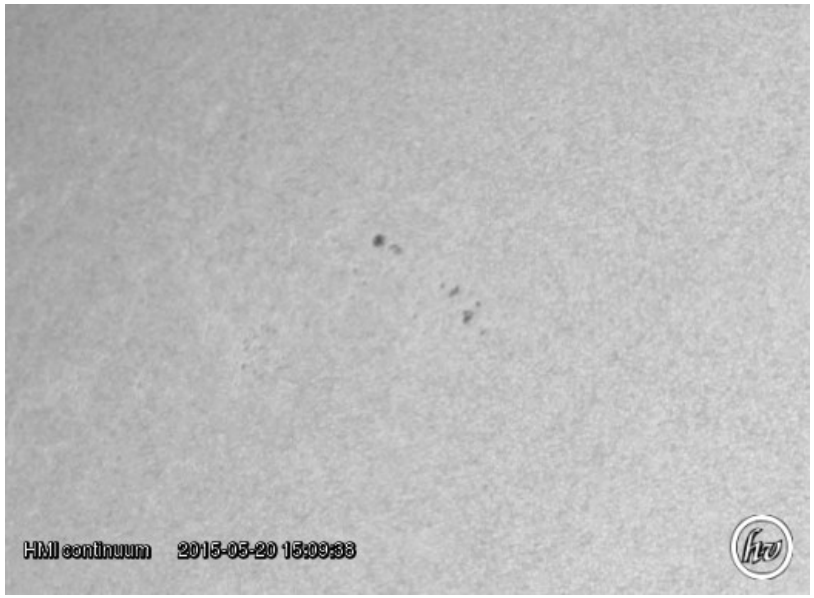

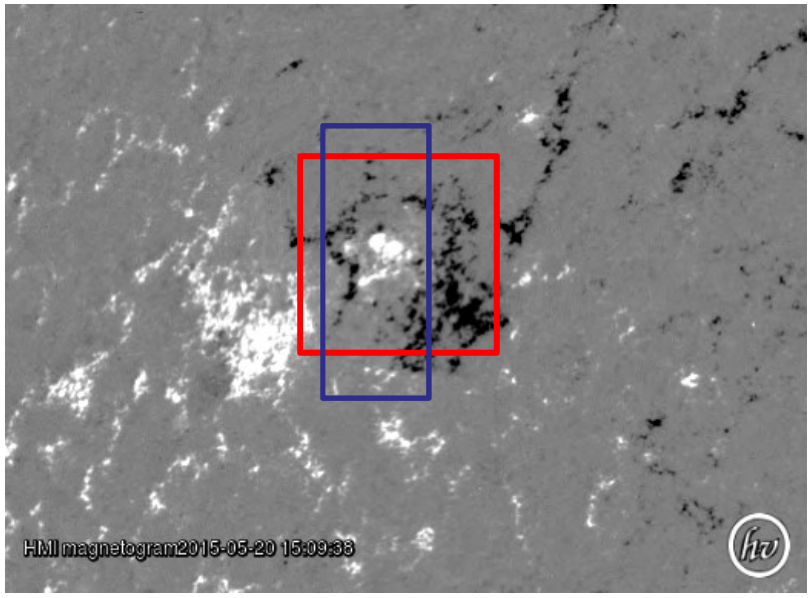

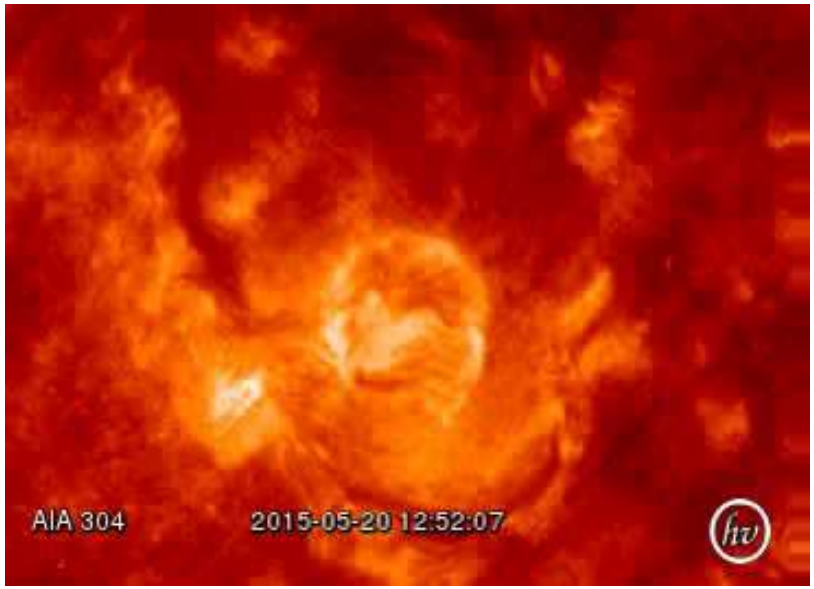

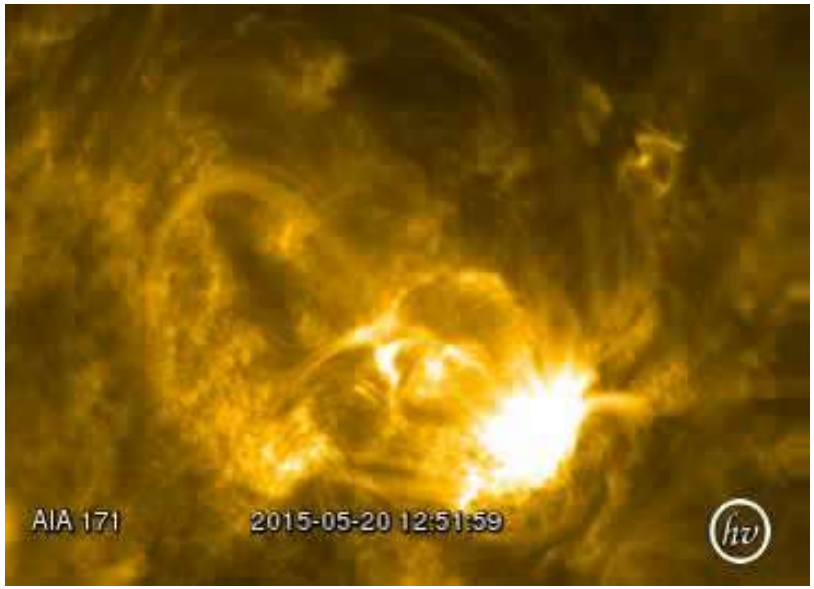

Fe I – 630.25 nm (IBIS)

Even if the seeing conditions were not very good, the IBIS FOV allowed us to see the main pore of the AR, in the center of the Fe I 630.25 nm line during the main phase of the flare, and another few smaller pores.

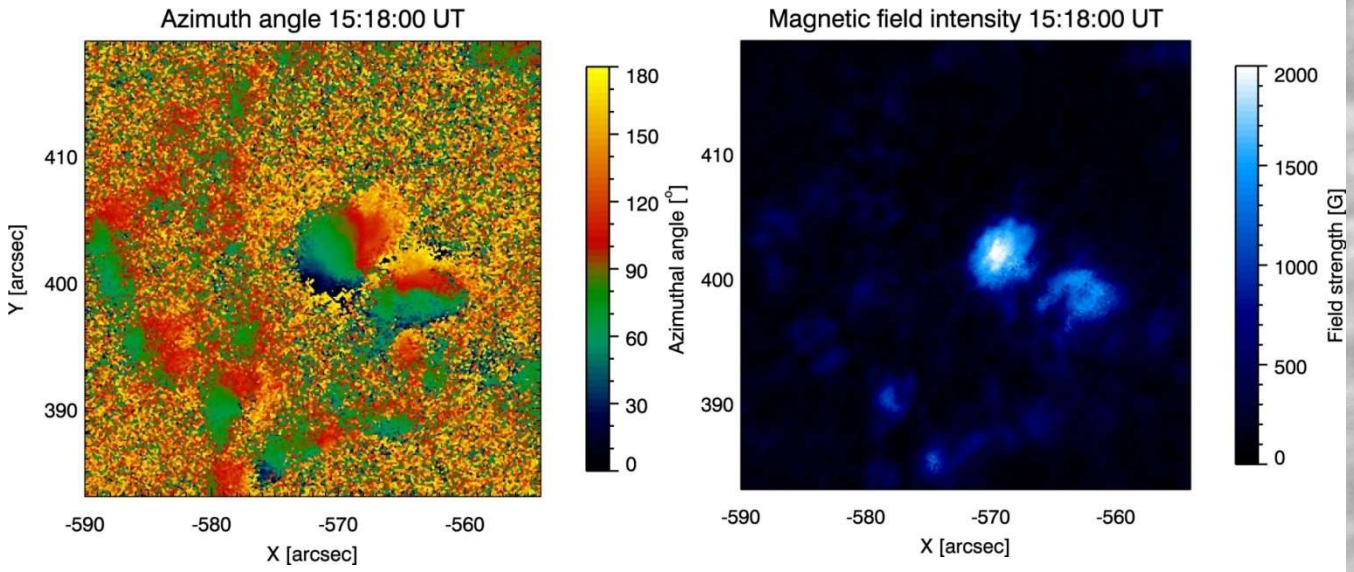

The magnetic field intensity in the main pore reaches 2000 G, while concentrations of the magnetic field above 1000 G correspond to the other smaller pores.

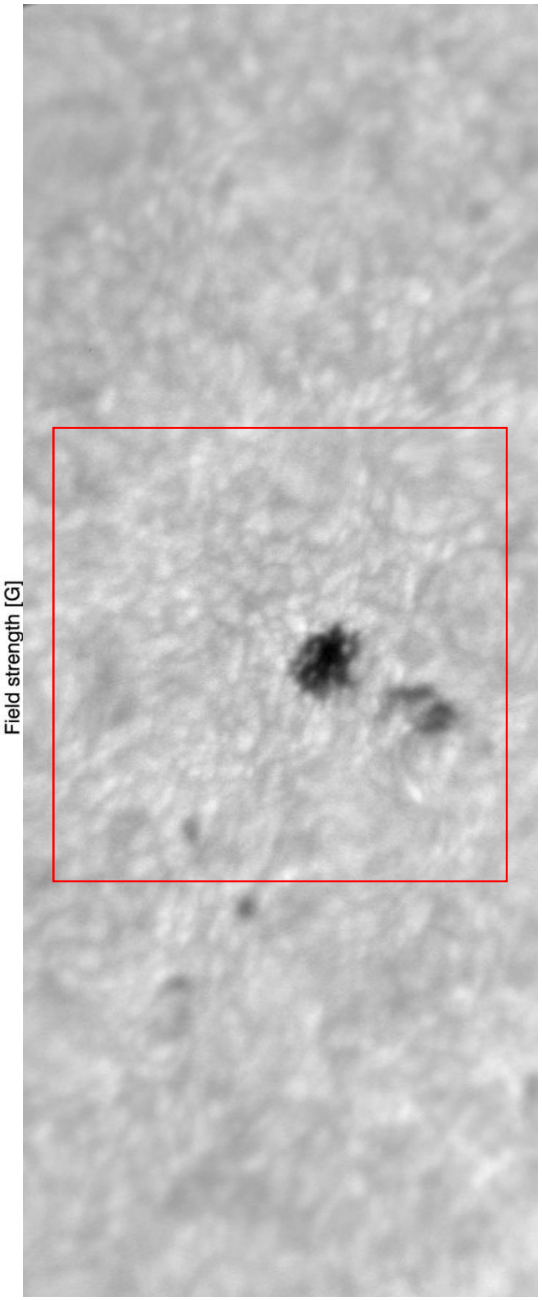

CaII – 854.2 nm (IBIS)

During the main phase of the flare, we observed part of the ribbons at the chromospheric level. At 854.2 nm we distinguish some small filaments connecting the main pore to the eastern surrounding ribbons.

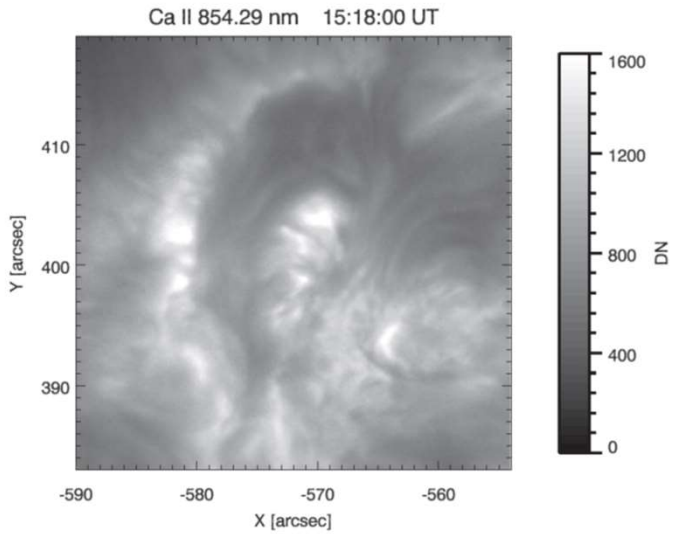

Although we were not able to observe the peak of the flare, we also saw some brightenings near the main pore, i.e., corresponding to the inner footpoints of these filaments.

However, the IBIS FOV does not allow us to see the entire surrounding ribbon and its shape.

Hβ 486.1 nm (ROSA)

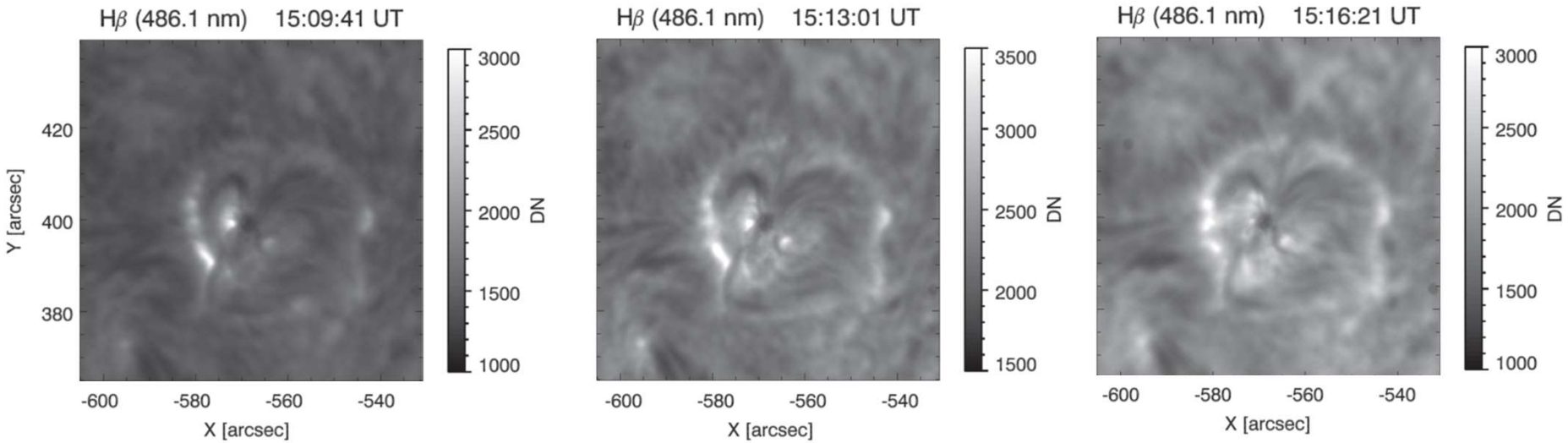

During the main phase of the flare, these footpoints start to brighten sequentially in a clockwise direction from the eastern to the western ones, producing a semicircular ribbon with a diameter of about 40″ and formed by several adjacent bright kernels of 1″–2″.

The brightenings were more intense at the outer footpoints of the darker filaments.

Halpha 656.28 nm (IBIS)

Pre-flare phase (from 14:19 UT)

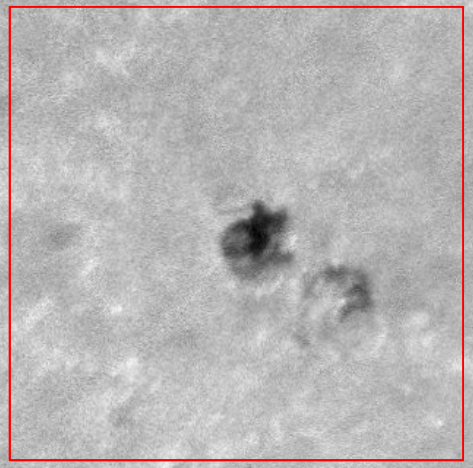

We reconstructed the profiles of the line in each spatial pixel by fitting the corresponding Stokes I component with a linear background and a Gaussian shaped line. The values of LOS velocity were deduced from the Doppler shift of the centroid of the line profiles in each spatial point with respect to the median of the centroid in the whole FOV.

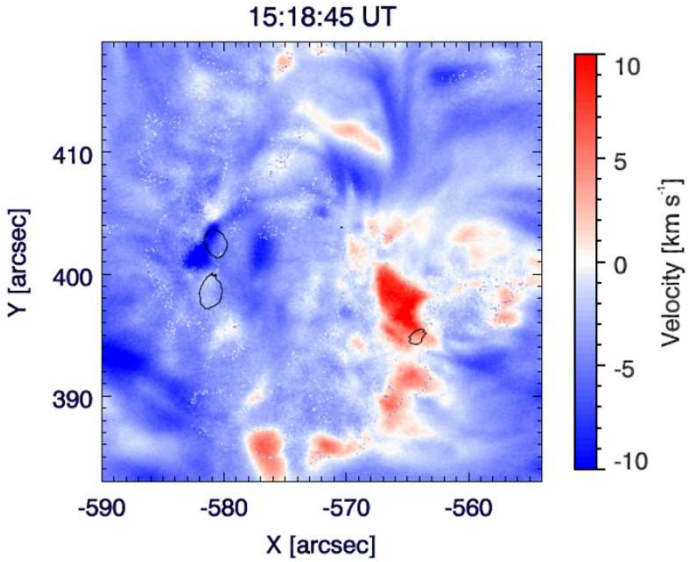

The darker filaments are characterized by a motion of the plasma toward the observer that is more intense than the background.
A blob of plasma located at [−567″, 397″] moves away from the observer.

Main phase (from 15:18 UT)

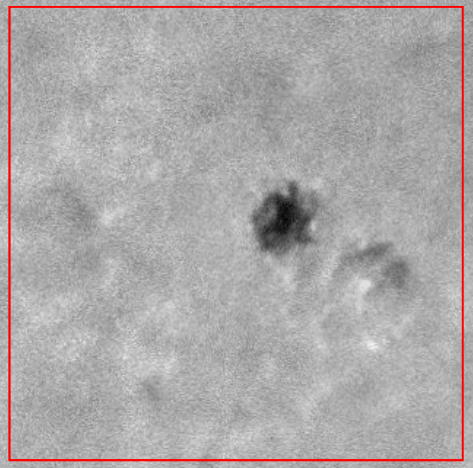

Null point

We considered the magnetogram acquired by HMI/SDO on 2015 May 20 at 14:22 UT as photospheric boundary conditions for the potential field extrapolation.

We also applied the method outlined in Beveridge (2006) to find the null points above the photospheric surface.

We found a null point located above the region of interface between the positive patches, corresponding to the smaller pores in the southern part of the IBIS FOV and the negative network of the supergranular cell.

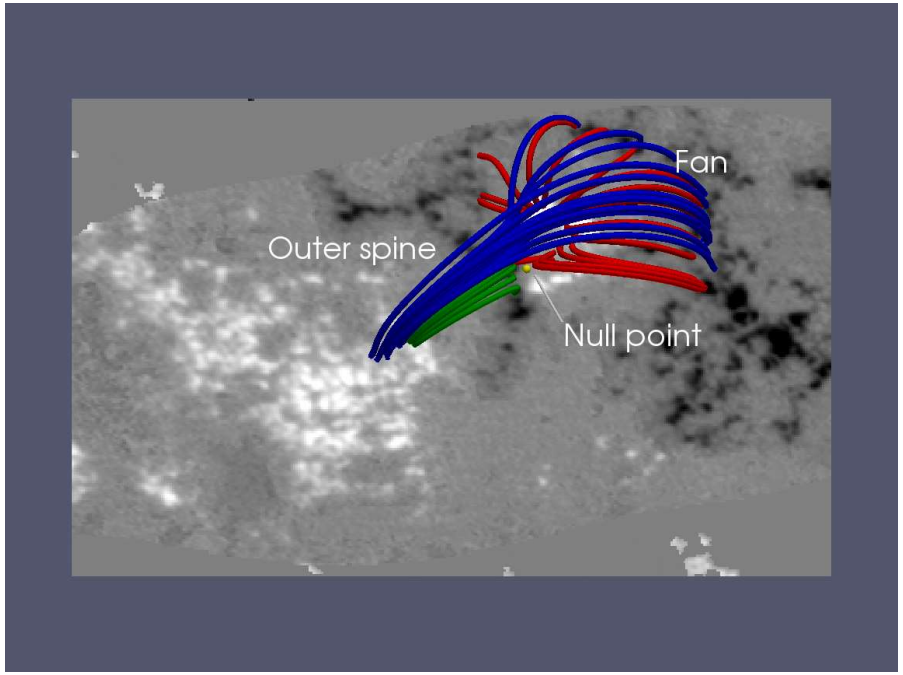

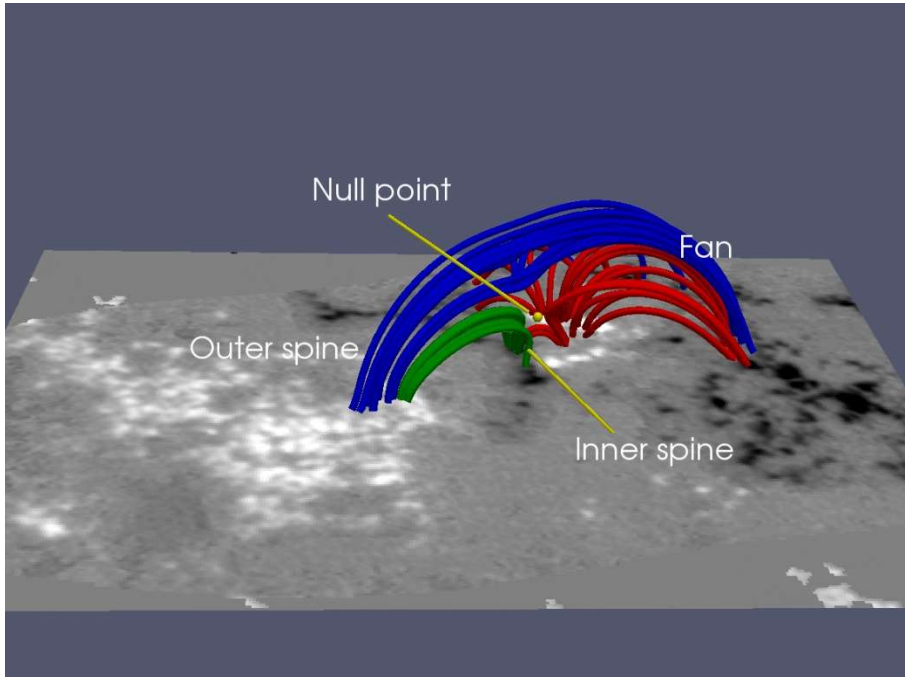

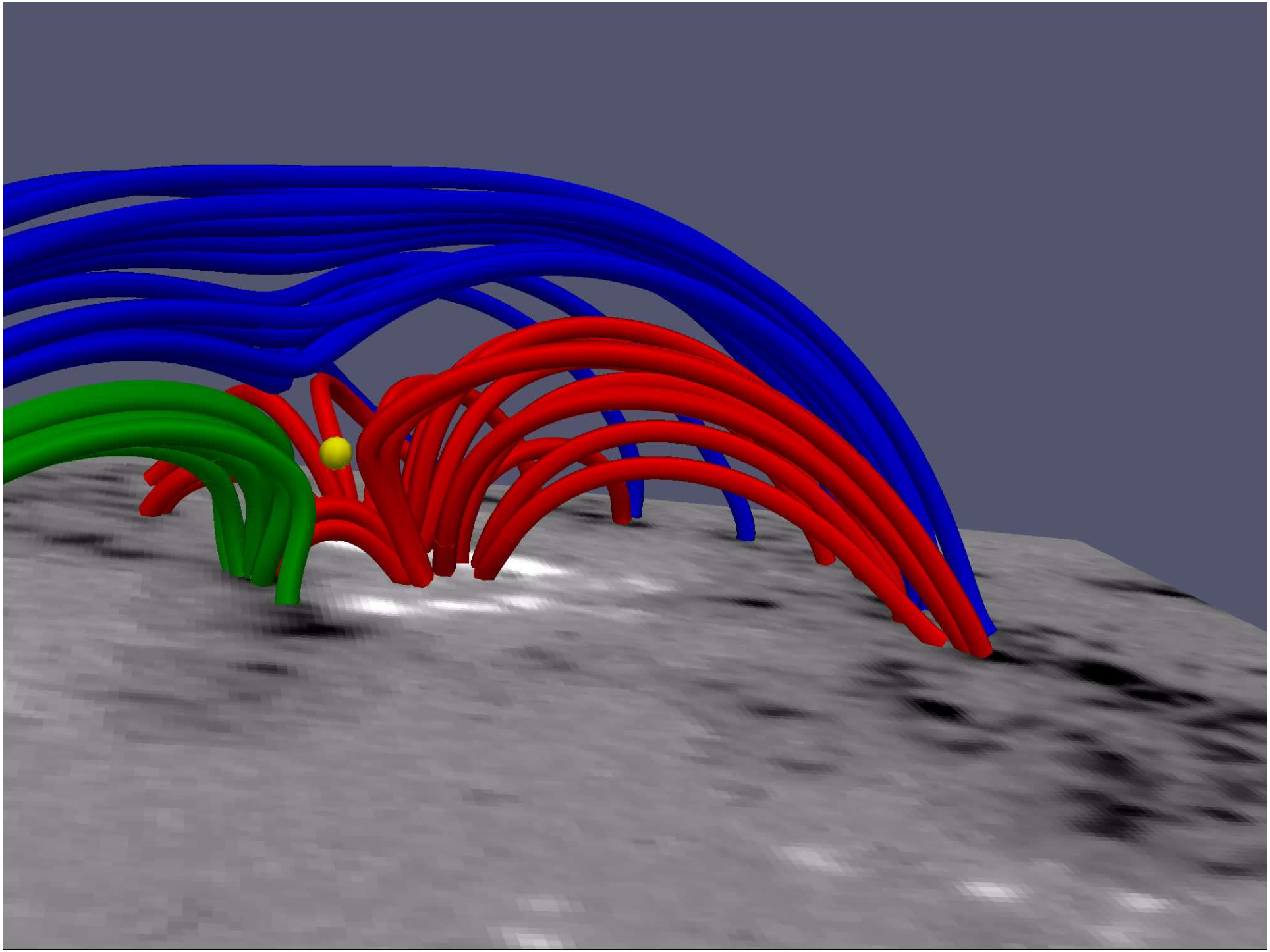

We estimated a ratio L/N of about **1.25**, where L is the distance between the footpoints of the coronal loop (about 50″), which became brighter at 171 Å a few minutes before the onset of the flare and N is the diameter of the semicircular ribbon (about 40″).
This ratio is the same taking into account the length of the outer spine and the fan loops in the potential field extrapolation.

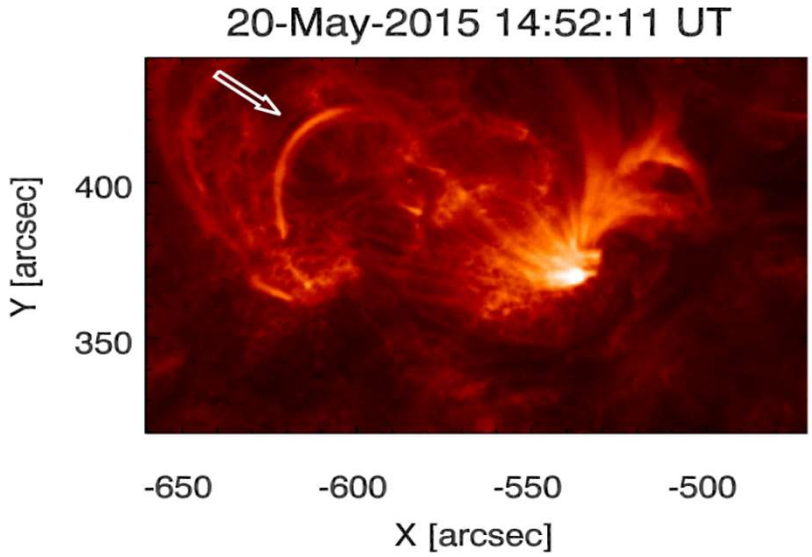

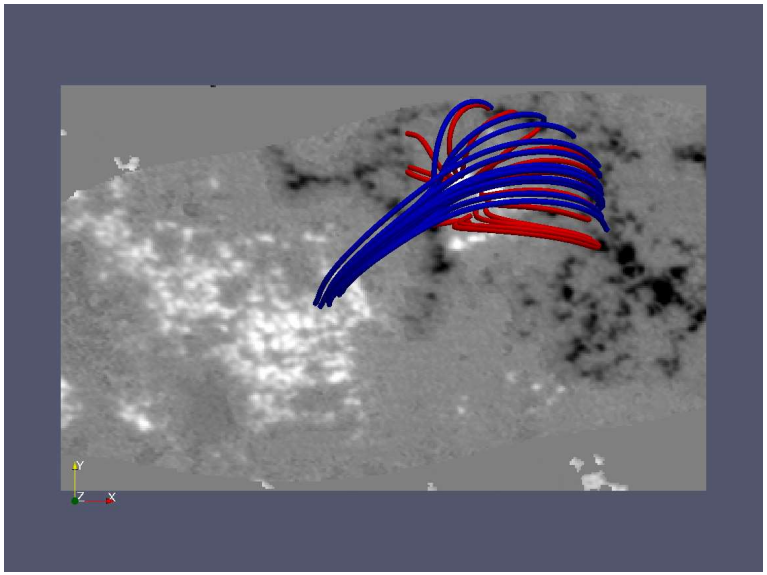

Therefore, the symmetry of the magnetic system may be responsible for the small amount of energy released during the flare.

RHESSI observed the flare

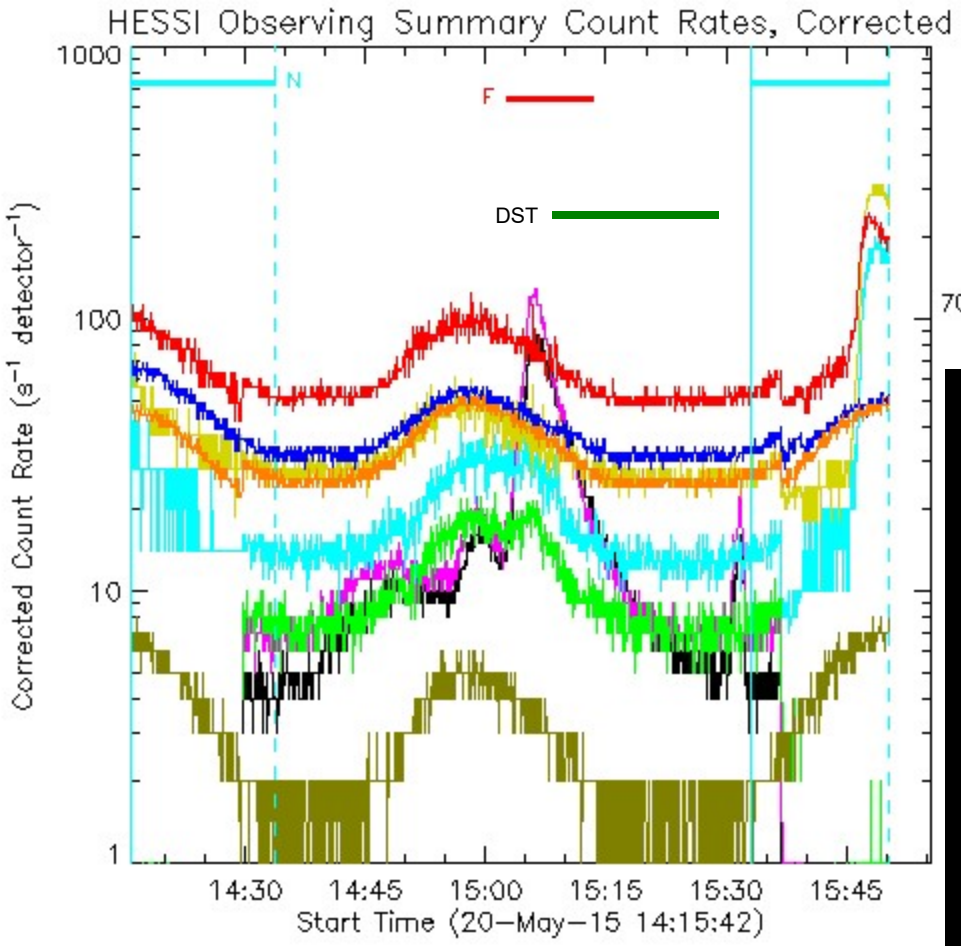

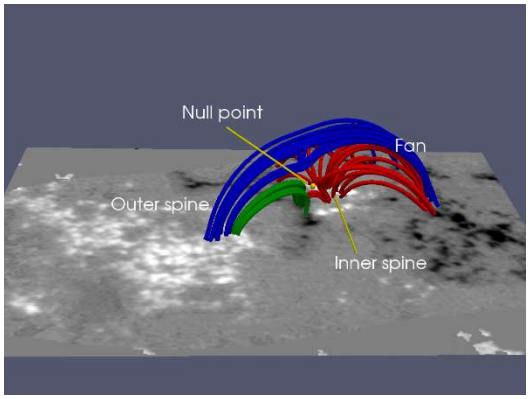

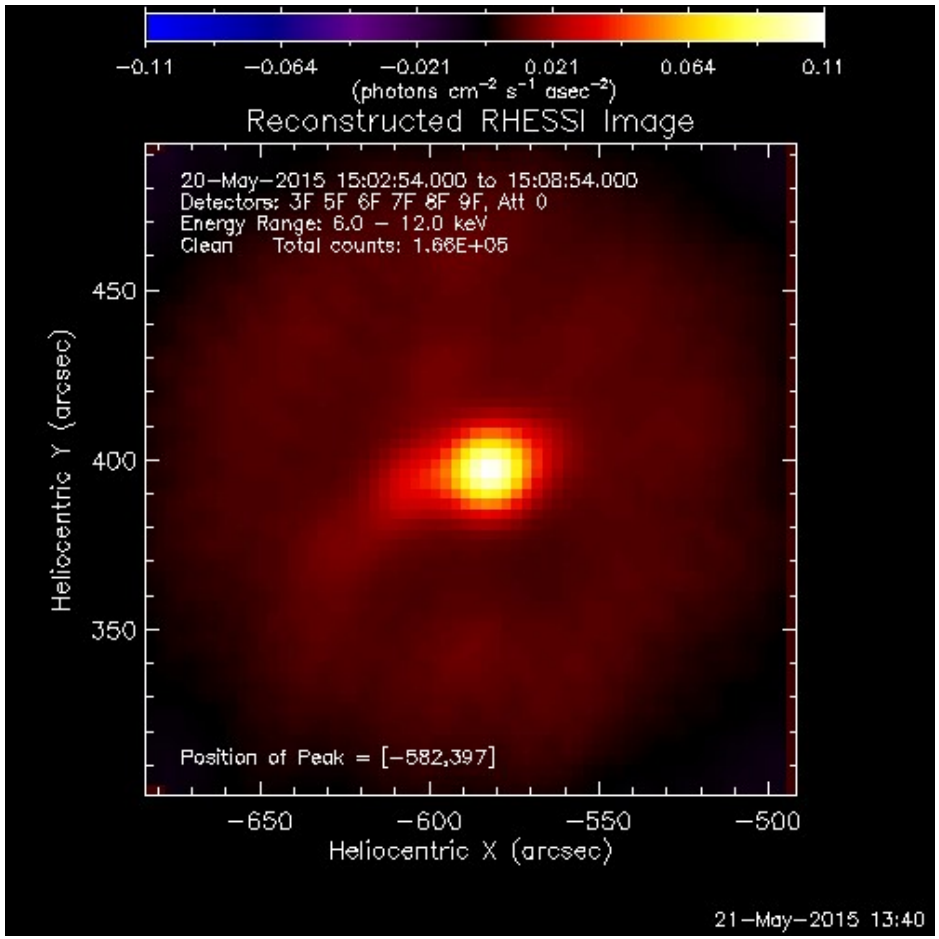

The site of the 3D null point and the shape of the outer spine were detected by RHESSI in the low-energy channel between 6.0 and 12.0 keV.

Conclusions

Loop corresponding to the outer spine became brighter a few minutes before the onset of the flare; then this kind of events may be preceded by **resistive instabilities along the spines.** The role of these instabilities should be investigated.

The circular ribbon was formed by several adjacent compact kernels characterized by a size of 1″–2″; the fact that the brighter ones correspond to the outer footpoints of the darker filaments is a signature of the **inhomogeneity** distribution of the magnetic field forming the fan.

These kernels started to brighten sequentially in clockwise direction (**slipping reconnection**).

We interpreted the filament material along the PIL not as being a single circular filament, but instead as being formed by **several filaments** connecting the main pore, in the center of the FOV, to the surrounding ribbons, along the same direction as the fan loops.

A new finding obtained from our study is that the new models of the magnetic reconnection around a 3-D null point should also take into account the **emission in the low energy X-ray** not only in the location of the null point but also along the outer spine.

The low intensity of this flare may be ascribed both to the low amount of magnetic flux involved in the event and the **symmetry** of the magnetic system.

How can EST help us to study such small / compact flares?

The EST shall provide the opportunity to deepen the observational aspects of these events by means of a wider sample of case studies and higher spatial and temporal resolution.

The maximum FOV in order to observe all the ribbons at the same time.

EST high polarimetric sensitivity should help to infer the magnetic field configuration in the outer solar atmosphere.

The high cadence of about 0.1 frame/s should allow to follow the temporal evolution of each ribbon.

Multi-wavelength observations at different height are useful to understand the deposition of accelerated particles along different paths in different magnetic domains.

Instrument 1	FP_vis, FP_ir	
Goal	Observe spectral lines formed at different heights in the chromosphere, from which temperature profile with column mass can be determined.	
	Requirement	Goal
Photosphere	Fe I 543.4	
Chromosphere	Ca II H 396.9 nm, Ca II 854 nm	+He I 1083 nm
Wavelength samples	0.01nm spectral resolution, across 0.3 nm spectral range	
FOV	60″ × 60″	120″ × 120″
Spatial resolution	0.″04	
SNR	200	
500 Cadence	5 s	1s
Notes	The focus here is only on I, hence low SNR requirement. To capture dynamical changes need to prioritise cadence. This observing program requires stable observations with AO locked, at different μ values.Photospheric line chosen as it is formed quite high in photosphere, bearing in mind likely range in height of strong perturbations caused by flare heating.	

Instrument 2	Broad-band Imagers	
Goal	High temporal and spatial resolution context observations of the flare ribbons.	
	Requirement	Goal
Photosphere	G-band	+CN Bandhead
Chromosphere	Ca II H line core and wing	+Hα
Wavelength samples	n/a	
FOV	60″ × 60″	120″ × 120″
Spatial resolution	0.″015	
SNR	> 100	
500 Cadence	1 s	0.1 s
Notes	For FOV, the tradeoff is between having a good chance of catching a flare (FOV) and highest possible spatial and temporal resolutions. The programme requires stable observations with AO locked at different μ values.	

Thank you for your attention!